Chemistry and Emissions of Nitrogen Oxides (NO, NO_2, N_2O) in Combustion of Solid Fuels II. Heterogeneous Reactions – N_2O

K. SVOBODA, J. ČERMÁK, and M. HARTMAN

Institute of Chemical Process Fundamentals, Academy of Sciences of the Czech Republic, CZ-165 02 Prague

Received 25 February 1999

Nitrous oxide (N_2O) volume fractions in atmosphere increase at an estimated rate 0.7—0.8 ppb per year. Potential anthropogenic sources of N_2O include fertilization, combustion, mobile (car) sources, and atmospheric transformation of NO_x to N_2O. Combustion of solid fuels and waste at lower temperatures (750—900 °C) presents a significant source of N_2O. During stages of a coal particle combustion (pyrolysis-devolatilization and char combustion) both volatile N and char N are mainly transformed to N_2 + NO and partly to N_2O. HCN was recognized as the main precursor of N_2O in volatile combustion. Char-N conversion to N_2O (through various mechanisms) is affected by *in situ* reduction of N_2O by carbon surface and CO.

Temperature has the most important effect on N_2O emissions. At temperatures over 1000 °C the N_2O emissions are negligible. Char and CaO are in practical combustion systems the most effective catalysts for thermal decomposition of N_2O.

Nitrous oxide (N_2O) has been identified as a contributor to the destruction of ozone in the stratosphere and recognized as a relatively strong greenhouse gas [1—4]. The anthropogenic contribution to the N_2O emission to the Earth atmosphere is estimated to be 5—7 × 10^6 ton/year. It is about 30—40 % of the total (natural + anthropogenic) N_2O emissions [1, 5]. The estimated components of N_2O emissions from human activities together with usual range of N_2O concentrations in off-gases are summarized in Table 1. The contributions of N_2O emissions from land cultivation by *N*-fertilizers and from atmospheric transformation of NO_x emissions including transformations in dry and wet depositions [1, 2, 6] are still only very roughly estimated. The simultaneous presence of NO, SO_2, O_2, and water either in the bulk liquid or adsorbed on solid surfaces has been confirmed [6] to produce significant levels of N_2O. Combustion of liquid and gaseous fuels at temperature over 1000 °C is not relevant as source of N_2O emissions. Low-temperature combustion (750—900 °C) of solid fuels (especially fluidized bed combustion) presents an important source of N_2O.

In combustion processes (for heat and energy production) practically only fluidized bed combustion (FBC) and noncatalytic selective NO_x reduction (NCSR) by NH_3 addition are important sources of N_2O emissions. The degree to which homogeneous and heterogeneous reactions contribute to N_2O formation in FBC depends on the combustion system arrangement, temperature, solid particle concentration, and on the particle catalytic properties in formation and destruction of N_2O.

Release of N_2O Precursors from Solid Fuels and Conversion of Volatile Nitrogen to N_2O

The coal (fuel) related factors considered to influence nitrogen oxide formation during combustion are as follows:

- coal structure, rank, volatile matter, fixed carbon and oxygen content,
- char structure and reactivity,
- total nitrogen content,
- nitrogen functionality in the coals, conversion to volatile nitrogen and char nitrogen.

The important factors, main routes leading to formation, interactions, and destruction of N_2O in coal combustion processes are schematically shown in Fig. 1. The oxidation reactions of volatiles may be homogeneous and/or heterogeneous, catalyzed by solid

Table 1. Estimates of Contributions of N_2O Emissions from Various Human Activities and N_2O Volume Fraction in Off-Gases

Source	Volume fraction contribution to the overall anthropogenic N_2O emissions/vol. %	Range of N_2O volume fractions in off-gases and in flue gas
Adipic acid production	5—8	30—50 vol. % !
Nitric acid production	4—7	300—3000 ppm
Land cultivation, fertilizers	10—45	
Fossil fuels (stationary)	4—10	40—400 ppm (fluidized bed combustion)
Fossil fuels (mobile)	4—15	0—800 ppm
Atmospheric transformation of NO_x and N_2O from dry and wet depositions	? (estim. 10—20)	
Waste incineration and biomass burning	? (estim. 5—15)	0—600 ppm
Selective catalytic reduction, noncatalytic selective reduction	?	10—150 ppm
Regeneration of catalyst from fluidized bed cracking in petrochemistry	?	?

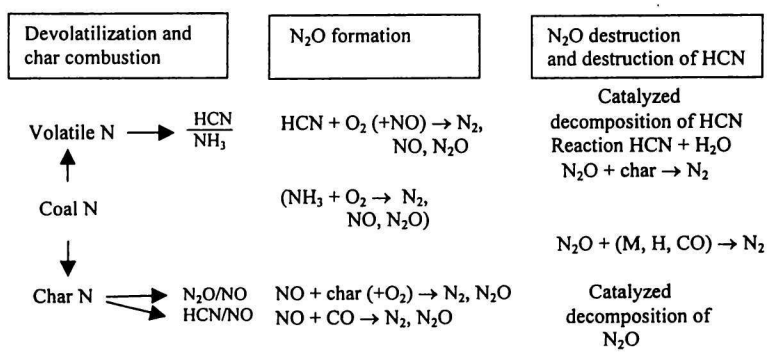

Fig. 1. Simplified reaction scheme for main factors influencing N_2O formation and destruction in combustion, especially in fluidized bed combustion.

particles and metallic surfaces. In systems with high particle concentrations (FBC) and lower temperatures the heterogeneous, catalyzed reactions are prevailing.

Nitrogen Functionality and Release of Ammonia and HCN during Pyrolysis and Gasification of Solid Fuels

Coals contain typically 1—2.5 mass % (daf) of nitrogen, peat contains 1—3 % N, and wood 0.1—0.7 % N. In coals according to rank and age the nitrogen is mostly bound in *N*-heterocyclic compounds (pyrrole and pyridine), a minor amount is bound in quaternary and amine functionalities. Almost 100 % of the nitrogen in peat and in wood is in the pyrrolic form. The concentration of pyridinic N (the probably most stable form from those) increases in the order [7]: wood, peat, lignite, bituminous coal, anthracite. It seems that the oxygen functionalities in solid fuels (—OH, —COOH, —C—O—, C=O groups and heterocyclic *O*-compounds) are not so stable as *N*-compounds and during pyrolysis/gasification of a solid fuel tend to split, react and escape sooner than *N*-compounds [8].

The enrichment of nitrogen in the char in pyrolysis reaches a maximum [9] in the temperature range 1000—1300 K. Further pyrolysis (at higher temperatures) results in the release of NH_3 and HCN, leading to a decrease in N/C relative mass fraction at higher temperatures. The type of nitrogen functionality and their molecular structures in coals are not factors determining the distribution of *N*-functionalities in chars. At lower temperatures the oxygen functionalities are associated with pyridone N and quaternary N in coals. The gradual conversion of pyrrolic nitrogen to pyridinic and quaternary N is a function of pyrolysis temperature, heating rate, and residence time. During the condensation process of pyrolysis the nitrogen atoms in char are incorporated into the graphene layers [9] (mostly as pyridinic and quaternary N). The mass percentage of coal nitrogen loss in pyrolysis and gasification in a fluidized bed (θ = 950 °C) is approximately linearly dependent on mass percentage of carbon loss [10].

The ratio of NH_3 to HCN in volatiles was recognized to be a very important factor from the point of view of further conversion to N_2O [1, 3, 11—13]. N_2O is mainly formed in volatile oxidation by oxidation of

Table 2. Conversions of Fuel Nitrogen to NH_3 and HCN in Slow (10 K min^{-1}) and Fast Pyrolysis (in N_2 at 910 °C) of a Peat and a Bituminous Coal [14] (Maximum Temperature 910 °C)

Fuel	w(Fuel nitrogen)	Mass ratio in fuel $m(O)/m(C)$	Conversion of fuel N to NH_3	Conversion of fuel N to HCN	Mole ratio $n(HCN)/n(NH_3)$
	mass %		%	%	
Peat, slow pyrolysis	2.8	0.627	21.5	2.5	0.115
Peat, fast pyrolysis			24	9	0.375
Coal, slow pyrolysis	2.2	0.0973	16	6	0.375
Coal, fast pyrolysis			14	4	0.24

HCN. Influence of heating rate and type of fuel (high and low content of oxygen) on yields of NH_3 and HCN [14] is given in Table 2.

The studies with wood, peat, coal, and model compounds [7, 15] have shown that conversion of fuel N to HCN and NH_3 depends on the $m(O)/m(N)$ or $m(O)/m(C)$ ratio in fuels. Increasing the $m(O)/m(N)$ ratio in fuels causes usually decreasing of the $n(HCN)/n(NH_3)$ ratio in gaseous product of pyrolysis, partial gasification, and generally in solid fuel devolatilization.

The $n(HCN)/n(NH_3)$ ratios in devolatilization are in a good correlation with the $n(N_2O)/n(NO)$ ratios measured in flue gas after combustion. Among oxygen groups in solid fuels especially the phenolic —OH group is very active in converting HCN to NH_3 during pyrolysis [7, 15].

In fluidized bed air gasification (with various air—water vapour mixture) the fuel N from solid fuels (wood, peat, and coals) is converted [16] from 30—90 % to NH_3. The conversions of fuel N to HCN are very low, only a few percent. Increasing temperature and decreasing operating pressure generally lead to higher HCN concentrations in air-water gasification. Longer residence time, larger coal particles, and slower heating rates usually cause the decrease of HCN concentrations.

Simple models of coal pyrolysis, gas and tar evolution (including evolution of HCN and NH_3) consider usually a simple equation [17] for the rate of volatiles or species evolved

$$dW_i/dt = \boldsymbol{k}_i \cdot (W_{0i} - W_i) \qquad (1)$$

where W_{0i} is the ultimate (total) yield of product (or gas) i ($m(i)/m(coal)$, and W_i is the amount of "i" already evolved.

Further assumption is frequently accepted that $\boldsymbol{k}_i$ is the rate constant given by the Arrhenius expression

$$\boldsymbol{k}_i = k_{0i} \cdot \exp(-E_{ai}/\boldsymbol{RT}) \qquad (2)$$

where k_{0i} is the frequency factor and E_{ai} is the activation energy for evolution of the species i.

Such models are directly applicable only to homogeneous systems with a single chemical process and single activation energy. However, because of simplicity, the model is used as well for more complicated processes of pyrolysis (with a number of reactions and a number of products) where the activation energy and frequency factor are not constant numbers in a temperature range.

Thermal dissociation of HCN to H + CN is becoming significant at very high temperatures (over 1500 °C). In systems with relatively low H_2 partial pressure NH_3 is catalytically decomposed to N_2 and H_2.

Conversion of Volatile Nitrogen to N_2O

After secondary pyrolysis of tar *N*-compounds in released volatiles, the most important precursors of nitrogen oxide emissions remain HCN and NH_3. In oxidation reactions of HCN and NH_3 generally both homogeneous and heterogeneous reactions take part [12, 13]. In the case of homogeneous oxidation reactions it was proved that oxidation of HCN and of mixtures (HCN + CO, HCN + NO) is the most significant source of N_2O. Homogeneous oxidation of NH_3 and of various mixtures (*e.g.* NH_3 + NO) has shown [12, 18] that conversions of NH_3 to N_2O were lower than 4 %.

In combustion systems with relatively higher concentrations of ash, lime/limestone, and char (like systems with fluidized bed combustion) and lower temperatures of combustion (below 1000—1100 °C) the heterogeneous catalytic reactions are at least concurring but mostly are prevailing (*i.e.* they are faster) over homogeneous reactions. The catalytic oxidation reactions leading to N_2O run concurrently with catalytic reactions of N_2O decomposition at higher temperatures. This fact presents significant obstacle in determination of "pure" kinetics of HCN oxidation to N_2O and selectivity of the conversion. The catalytic oxidation of HCN over calcined limestone to NO and N_2O and corresponding selectivities σ for NO and N_2O formation from HCN are shown in Fig. 2.

Moreover, nitric oxide (created either by HCN oxidation or added from other sources) can react with HCN to N_2 and N_2O causing lower selectivities for NO formation and higher selectivities for N_2O [13]. In the presence of higher H_2O concentrations and lower O_2 concentrations a significant part of HCN (3—10 %) is

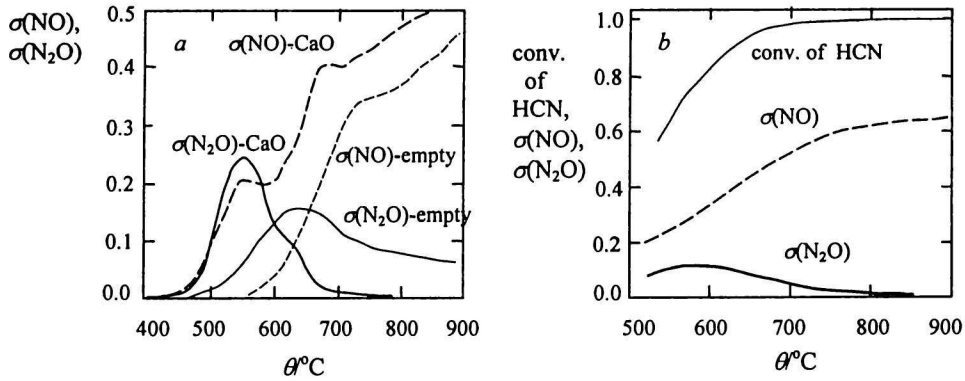

Fig. 2. *a*) Catalytic influence of CaO on HCN oxidation to NO and N_2O in a fixed bed quartz reactor [19]. Heating rate 3 K min^{-1}, inlet gas volume fraction 813 ppm HCN, 6 vol. % O_2, N_2 to the balance. 1.5 g of limestone particles (0.2—0.3 mm). *b*) Influence of temperature on selectivities in HCN oxidation over calcined, reactive limestone (chalk) [13], mass of limestone 0.24 g (0.25—0.3 mm). Inlet gas volume fraction 290 ppm HCN, 1 vol. % O_2, effect of N_2O decomposition not corrected. $\sigma(NO)$, $\sigma(N_2O)$ = selectivities for NO and N_2O formation in HCN oxidation. Conversion of HCN = $(n(HCN)_{in} - n(HCN)_{out})/n(HCN)_{in}$.

converted to NH_3 [20, 21], which further contributes to reduction of N_2O emissions and the conversion selectivities.

The reaction order with respect to HCN in lime-catalyzed oxidation reaction was found to be one [22] or less than one [13]. The reaction constant k_{kin} (per mass unit of catalyst – CaO) for lime-catalyzed HCN oxidation according to the equation

$$-r(HCN) = k \cdot c(HCN) \cdot c(O_2) = k_{kin} \cdot c(HCN) \quad (3)$$

at 1100 K is in the range 1—10 $m^3\ s^{-1}\ kg^{-1}$.

The mechanism of HCN oxidation in gas phase to N_2, NO, and N_2O seems to involve the following reactions

$$HCN + O^{\bullet} \rightarrow NCO^{\bullet} + H^{\bullet} \quad (A)$$

$$HCN + OH^{\bullet} \Leftrightarrow CN^{\bullet} + H_2O \quad (B)$$

$$CN^{\bullet} + OH^{\bullet} \rightarrow NCO^{\bullet} + H^{\bullet} \quad (C)$$

$$NCO^{\bullet} + H^{\bullet} \rightarrow NH^{\bullet} + CO \quad (D)$$

$$NH^{\bullet} + (HO_2)^{\bullet} \rightarrow NO + H_2O \quad (E)$$

$$CO^{\bullet} + NO \rightarrow N_2O + CO \quad (F)$$

$$NH^{\bullet} + NO \rightarrow N_2O + H^{\bullet} \quad (G)$$

The $CN^{\bullet}$, $NCO^{\bullet}$, and $NH^{\bullet}$ are the most important *N*-intermediate products.

The formation of N_2O is immediately followed by destruction reactions

$$N_2O + (H^{\bullet}, OH^{\bullet}, M) \rightarrow N_2 + (OH^{\bullet}, (HO_2)^{\bullet}, O^{\bullet}) \quad (H)$$

In the presence of solid particles the radicals are "quenched" on solid surfaces and the mechanism is changed to Langmuir—Hinshelwood adsorption-reaction kinetics. The knowledge of surface, catalytic mechanism of N_2O formation remains still incomplete.

The selectivities for N_2O formation at temperatures over 1000 K are only a few percent (due to rapid N_2O-catalyzed decomposition). In laboratory experiments with coal combustion in a fluidized bed of quartz particles at temperatures between 800 °C and 900 °C [23] and 5 vol. % O_2 typically 2—10 mass % of volatile nitrogen was converted to N_2O and 20—40 mass % of volatile N was converted to NO. Bituminous and anthracitic coals with low content of volatile may exert relatively very high conversions [23] of volatile N to N_2O (20—30 mass %). The reason is probably in higher $n(HCN)/n(NH_3)$ ratio, lower H_2O concentration in volatiles and flue gas, lower ash content, *etc.* During dynamic process of coal devolatilization and volatile combustion of larger coal particles ($\approx$ 10 mm) in the fluidized bed the $\varphi(N_2O)/\varphi(NO)$ emission ratio remains usually relatively constant [23], strongly dependent on coal rank and operating temperature. Increasing temperature of combustion has the biggest effect on destruction of N_2O. In combustion processes at temperatures over 950 °C the emissions of N_2O are generally very low or neglectable.

In the homogeneous oxidation of NH_3 below 1000 °C measured N_2O concentrations were near zero [24]. Between 1000 °C and 1100 °C the conversions to N_2O were less than 4 %. The necessary condition for N_2O formation was the presence of NO in the system. For systems with solid particles and dust the N_2O formation (corrected for catalytic N_2O decomposition) was reported to attain the maximum values for N_2O selectivity about 4 %. At higher temperatures the catalytic decomposition of N_2O prevails. Formation of N_2O over sulfated limestones has been found to be negligible [12].

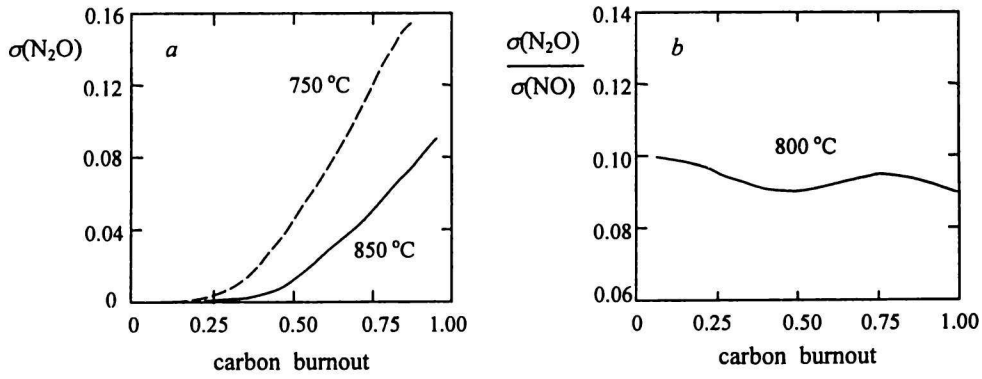

Fig. 3. *a*) Effect of temperature on the selectivity $\sigma(N_2O)$ for N_2O formation from char N during combustion of a coal char (91.9 % C, 1.3 % N, 3.6 % O) [25]. Volume fraction of O_2: 14 vol. %, fixed bed reactor, 0.5 g of char (d_p = 0.18—0.22 mm) with freeboard for homogeneous reactions among gases. *b*) Ratio of selectivities for NO and N_2O formation from char N [26] in a fixed bed char combustion (d_p = 0.25—0.355 mm), bed height 20 mm, char load 15 mg, inlet O_2 concentration 3.5 %, gas residence time within the bed 60 ms.

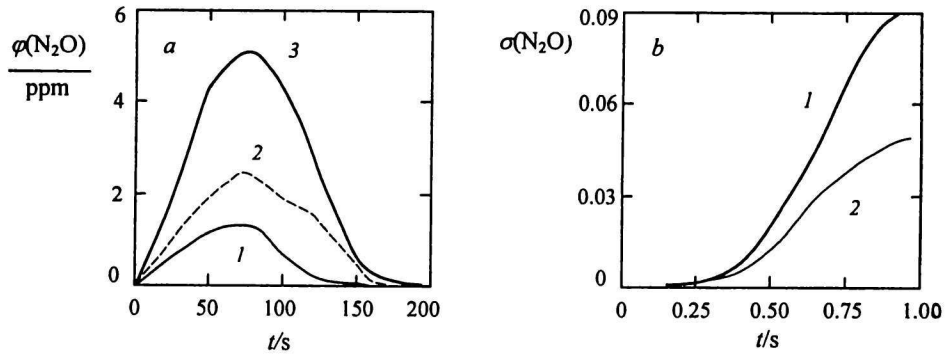

Fig. 4. *a*) N_2O formation from fixed bed combustion of chars [25] prepared at different temperatures. Conditions: size of char particles 0.18—0.22 mm, inlet O_2 volume fraction 1 vol. %, temperature 800 °C. *1.* Char prepared at 1000 °C (residual volatile content 0.5 mass %); *2.* char prepared at 800 °C (residual volatile content 2 mass %); *3.* char prepared at 700 °C (residual volatile content 4 mass %). *b*) Selectivity for N_2O formation in char combustion with (*1*) and without (*2*) NO addition (char particles 91.9 mass % C, 1.3 mass % N, 3.6 mass % O) [25]. Combustion temperature 800 °C, fixed bed reactor [25] without homogeneous reactions after fixed bed combustion, inlet gas volume fraction of O_2 14 vol. %, NO 242 ppm.

Oxidation of Char Nitrogen to N_2O

Experimental Results on Char-Nitrogen Oxidation to N_2O

Char nitrogen is released during char oxidation mainly as N_2 and NO, partly as N_2O, HCN, and NH_3. The fractional conversions of char N to NO and N_2O are roughly proportional to carbon burnout both in fixed and fluidized bed combustion [12, 25, 26]. The measured fractional conversions of char N to N_2O are in the range 1—16 % according to temperature, O_2 concentration, coal rank, particle size, char properties, combustion system, *etc.* Typical experimental results on char N to N_2O conversions measured in a laboratory fixed bed combustion are reported in Fig. 3.

Increasing temperature of combustion causes generally a strong decrease of N_2O emissions. It has to be stressed, however, that char pore surface reacts with evolved NO and N_2O. Char is very active in reduction of N_2O and therefore the measured N_2O emissions are affected by this *in situ* reduction [12]. Reduction of N_2O takes place in two different ways: within char pore system (during diffusion of N_2O to the char surface) and by contact with other char particles (*e.g.* in a fixed bed).

Char pyrolysis/gasification conditions (temperature, heating rate, residual content of volatiles) influence N_2O formation in char combustion (see Fig. 4). The higher the residual volatile content in a char, the higher conversion of char N to N_2O has been found [25]. It implies that increasing the devolatilization (pyrolysis, gasification) temperature of a char usually decreases N_2O formation.

Coal rank substantially affects N_2O formation from char combustion. The char N→ N_2O conversions in-

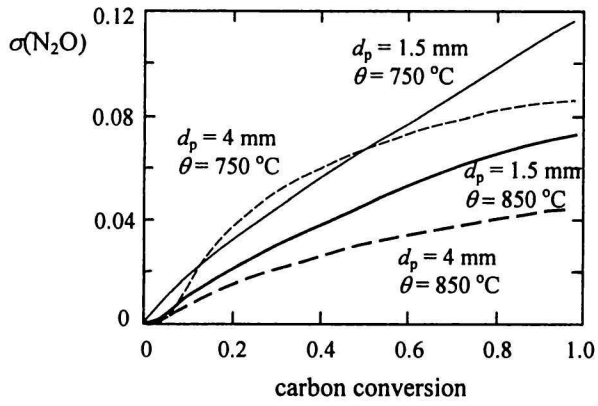

Fig. 5. Selectivity $\sigma(N_2O)$ for N_2O formation from coal N in fluidized bed combustion at temperatures 750 °C and 850 °C as a function of carbon conversion [28]. Size of coal particles: 1.5 and 4 mm. Volume fraction of oxygen: 4 vol. %.

crease usually in the order: peat, lignite, subbituminous coals, bituminous coals, anthracite and pet-coke.

The increasing of gas phase oxygen concentrations usually causes higher N_2O emissions, but simultaneously the effect of O_2 concentration on temperature of burning char particles has to be taken into account (*i.e.* higher char temperature at higher oxygen concentrations and as a consequence a higher kinetic rate of N_2O destruction).

NO addition to inlet gases entering a combustion system leads to elevation of N_2O emission [25] as shown in Fig. 4*b*. The reaction of nitric oxide (NO) with char N may follow various, different mechanisms as it was confirmed [27] by isotope marked ^{15}NO. Nitrous oxide (N_2O) was proved to be formed from char ^{14}N and gaseous, added ^{15}NO (like $^{14}N^{15}NO$) and from ^{15}NO nitrogen only (like $^{15}N_2O$).

Dependence of N_2O emissions on char particle size depends on coal rank, oxygen concentration, and temperature. The most observed trend [28] is decreasing of char N to N_2O conversions with increasing char particle size, as illustrated in Fig. 5.

At lower oxygen concentrations and at substoichiometric combustion conversions of char N to HCN and NH_3 have been measured [12], but always only small values (1—10 %). Such released HCN and NH_3 are subjected to homogeneous and heterogeneous, catalytic reactions further in a gas "film" surrounding char particles and in the "bulk" of gas phase.

Mechanism and Modelling of Char-Nitrogen Oxidation to N_2O

Mechanism of N_2O and NO formation from char N in combustion is still subject of discussions. As it was suggested in literature and proved experimentally [27, 29, 30], three mechanisms are possible for char-N transformation into N_2O.

Mechanism I: Direct oxidation of char nitrogen. Final reaction of two adjacent nitrogen sites (partly oxidized) in the char matrix results in N_2O

$$O_2 + (—C) + (—CN) \rightarrow (—CO) + (—CNO) \qquad (I)$$

$$(—CNO) \rightarrow NO + (—C) \qquad (J)$$

$$(—CN) + (—CNO) \rightarrow N_2O + 2(—C) \qquad (K)$$

This mechanism is probably valid for combustion under slightly substoichiometric reaction conditions for reaction of O_2 with char + char N and for relatively short contact time of released NO (reaction (*13*)) with char surface. The probability of simultaneous reaction of two active sites containing nitrogen is relatively small, but nonzero.

Mechanism II: Reaction of gaseous NO with char nitrogen (both in the presence and absence of oxygen in gas phase) [29, 30]

$$NO + (—CNO) \rightarrow N_2O + (—CO) \qquad (L)$$

$$NO + (—CN) \rightarrow N_2O + (—C) \qquad (M)$$

but in the absence of oxygen the direct reduction of NO by (—C) is preferred and N_2O reacts as well with (—C)

$$NO + (—C) \rightarrow 1/2N_2 + (—CO) \qquad (N)$$

$$N_2O + (—C) \rightarrow N_2 + (—CO) \qquad (O)$$

NO in gases containing O_2 may even be adsorbed onto char surface and further react with gaseous NO, as it was proved [27] by isotopically labelled ^{15}NO, which formed by contact with char both $^{14}N^{15}NO$ and $^{15}N_2O$.

Mechanism III: The devolatilization or gasification of char nitrogen leads [29, 30] to formation of HCN and NH_3 as nitrogen intermediates followed by gas phase, mostly homogeneous, oxidation through reactive radicals ($NCO^{\bullet}$, $HNCO^{\bullet}$, $NH^{\bullet}$, *etc.*) to N_2, NO, and N_2O. The mechanism of gas phase oxidation may be governed by radical reactions (as described *e.g.* in eqns (*3*) and (*A*—*G*)) or by catalyzed reactions. Which mechanism, from those above, will prevail depends on reacting conditions (oxygen concentration, gas phase composition, temperature), char properties (reactivity, residual volatile content, oxygen content, particle size, *etc.*), and on combustion system (fixed bed, fluidized bed, entrained flow, *etc.*). Summary of kinetic constants for important reactions of char oxidation and char-N oxidation leading to N_2, NO, and N_2O is given in Table 3.

The mole fractions of individual active sites (x_S) in Table 3 are defined as

Table 3. Values of Relevant Kinetic Constants ($k_{kin} = A \cdot \exp[-E_a/RT]$) for Reactions at Temperatures 1000—1300 K. The NO and N_2O Relevant Kinetics is Based on Data for a Lignite [30]

Reaction and rate expression	E_a/(kJ mol^{-1})	Pre-Exponential factor A	Ref.
Char oxidation to CO $2C + O_2 \rightarrow 2CO$ $r_v = k_{kin} \cdot c(O_2)$ mol m^{-2} s^{-1}	90	$0.554 \times \{T_p\}$ $\frac{m^3}{m^2\ s}$	[20]
Oxidation of CO in the presence of H_2O $CO + 1/2O_2 \rightarrow CO_2$ $r_v = k_{kin} c(CO)(c(O_2))^{0.5}(c(H_2O))^{0.5}$ mol m^{-3} s^{-1}	125.5	3.25×10^7 m^3 mol^{-1} s^{-1}	[20]
Dissociative adsorption of O_2 $O_2 + 2(—C) \rightarrow 2(—CO)$ $r_v = k_{kin}\ x_S(—C)^2\ p(O_2)$ kg m^{-2} s^{-1}	42	8×10^{-7} kg m^{-2} s^{-1} Pa^{-1}	[30]
Desorption of CO $(—CO) \rightarrow CO$ + free site $r_v = k_{kin}\ x_S(—CO)$ kg m^{-2} s^{-1}	47	9×10^{-2} kg m^{-2} s^{-1}	[30]
Oxidation of char-C and char-N surface $O_2 + (—C) + (—CN) \rightarrow$ $(—CO) + (—CNO)$ $r_v = k_{kin}\ x_S(—C)\ x_S(—CN)\ p(O_2)$ kg m^{-2} s^{-1}	58	12×10^{-6} kg m^{-2} s^{-1} Pa^{-1}	[30]
Release of NO from char $(—CNO) \rightarrow NO + (—C)$ $r_v = k_{kin}\ x_S(—CNO)$	40	14×10^{-2} kg m^{-2} s^{-1}	[30]
Reaction between NO and oxidized char N $NO + (—CNO) \rightarrow N_2O + (—CO)$ $r_v = k_{kin}\ x_S(—CNO)\ p(NO)$	120	4 kg m^{-2} s^{-1} Pa^{-1}	[30]
Reduction of NO on *C*-sites $NO + (—C) \rightarrow 1/2N_2 + (—CO)$ $r_v = k_{kin}\ x_S(—C)\ p(NO)$	65	1×10^{-6} kg m^{-2} s^{-1} Pa^{-1}	[30]
Reduction of N_2O on *C*-sites $N_2O + (—C) \rightarrow N_2 + (—CO)$ $r_v = k_{kin}\ x_S(—C)\ p(N_2O)$	72	4×10^{-5} kg m^{-2} s^{-1} Pa^{-1}	[30]

$$x_S(C) = n(—C)/S, \quad x_S(—CO) = n(—CO)/S$$

$$x_S(—CN) = n(—C)/S \qquad (4)$$

$$x_S(—CNO) = n(—CNO)/S$$

4 and the sum S of all active sites in a char is assumed to be

$$S = n(—C) + n(—CO) + n(—CN) + n(—CNO) \quad (5)$$

Mechanism of char oxidation (Table 3) is changing in the temperature range 1000—1300 K. This is the main reason for the fact that the frequency (pre-exponential) factor is commonly used as a linear function of temperature in reaction rate equations for char oxidation in broader temperature range.

In the reaction rate expression for CO oxidation in Table 3, H_2O is involved, because the CO oxidation has a more complicated (chain) character with significant role of OH$^\bullet$ radicals, especially at higher temperatures in the presence of water vapour. These OH$^\bullet$ radicals are closely related to water vapour concentration. The equation for CO oxidation given in Table 3

Table 4. Evaluated Kinetic Data (Activation Energies and Pre-Exponential Factors) for Catalytic Decomposition of N_2O over Calcined Limestone and Coal Ash [31]

Catalyst	Frequency factor, k_0	Activation energy, E_a	Temperature range	Ref.
	$m^3\ kg^{-1}\ s^{-1}$	kJ mol^{-1}	°C	
Calcined limestone	2.3×10^3	68.2	700—850	[31]
Calcined limestone	4.3×10^3	68.2	650—850	[31]
Calcined chalk	1.3×10^6	110	700—850	[31]
Coal ash (inert conditions)	$1.4—17 \times 10^5$	170—185	700—850	[31]
Peat ash	5.3×10^8	200—215	750—900	[34]

is recommended, reasonable approximation [20] of a more complex kinetics.

Catalytic Decomposition and Reduction of Nitrous Oxide (N_2O)

Catalytic Decomposition of Nitrous Oxide

Various coal ashes, calcined limestone [31], metallic oxides (CaO, Fe_2O_3, CuO, and Ni, Co, Cr, Mn, Ln oxides and their mixtures), spinels, silicates, oxide mixtures of perovskite types, various noble metals [32], and zeolites (especially Cu, Co, Fe ZSM-5 zeolites) [32, 33] were recognized to be catalytically active in decomposition of N_2O to N_2 and O_2. The highest catalytic activities are exhibited by oxides of transition metals (Rh, Ir, Co, Fe, Ni), Cu, La, and alkaline earth (Ca, Sr) [32]. The apparent activation energies in Arrhenius equation for N_2O decomposition range between 80—170 kJ mol^{-1} for pure metal oxides. Perovskites and ion-exchanged zeolites exert often lower values of activation energies (30—50 kJ mol^{-1}). Typical measured values of frequency (pre-exponential) factor and apparent activation energy for calcined limestones and coal ash [31] are reported in Table 4. Presence of other adsorbing (interfering) gases causes generally changes in activation energies. *E.g.* for ion-exchanged ZSM-5 zeolites the evaluated activation energies in various gas mixtures are given in Table 5.

Mechanism of catalytic destruction of N_2O is usually supposed to be composed of three or four basic steps

$$N_2O + A^* \underset{k_{-1}}{\overset{k_1}{\rightleftharpoons}} N_2O^* \qquad (6)$$

$$N_2O^* \xrightarrow{k_2} N_2 + O^* \qquad (7)$$

$$2O^* \underset{k_{-3}}{\overset{k_3}{\rightleftharpoons}} O_2 + 2A^* \qquad (8)$$

$$N_2O + O^* \xrightarrow{k_4} N_2 + O_2 + A^* \qquad (9)$$

Table 5. Changes in Activation Energies of N_2O Decomposition (1000 ppm) in Various Gas Mixtures over ZSM-5 Zeolites [32]

Zeolite	Apparent activation energies/(kJ mol^{-1})		
	only N_2O	$\varphi(CO)/\varphi(N_2O) = 2$	3 vol. % O_2
Co	110	115	118
Cu	138	187	170
Fe	165	78	187

where A*, N_2O^*, and O* denote free catalyst active site, active site with adsorbed N_2O, and active site with atomic oxygen, respectively.

The total sum of mole fractions of active sites x_A, x_O, x_{N_2O} is supposed to be one

$$1 = c(A^*)/c(N_T) + c(O^*)/c(N_T) + c(N_2O^*)/c(N_T) = \\ = x_A + x_O + x_{N_2O} \qquad (10)$$

where $c(A^*)$, $c(O^*)$, $c(N_2O^*)$, and $c(N_T)$ denote the molar concentration of active sites A*, O*, N_2O^*, and the total active site concentration per volume unit of catalyst (in mol m^{-3}), respectively.

If eqn (7) is the rate-determining step, the reaction of N_2O with O* is neglected and steady state of active sites is assumed, the following equation can be derived [5] for the rate of N_2O decomposition $-r(N_2O)$

$$-r(N_2O) = k_2 \cdot (k_1/k_{-1}) \cdot c(N_T) \cdot p(N_2O)/ \\ \{1 + (k_1/k_{-1}) \cdot p(N_2O) + [p(O_2)/(k_3/k_{-3})]^{0.5}\} \qquad (11)$$

For practical cases (low N_2O concentrations) the rate equation (*11*) is of the first order (or with reaction order slightly below one) with respect to N_2O partial pressure. The reaction order with respect to oxygen is typically between 0 (for low oxygen partial pressures) and −0.5 (for higher O_2 partial pressures).

The catalytic activity of calcined limestone for N_2O decomposition decreases with increasing concentration of CO_2 and at lime recarbonation or sulfation

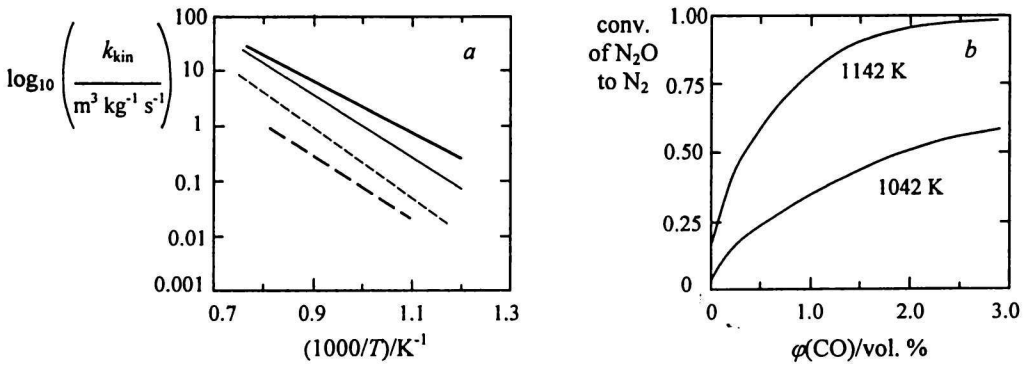

Fig. 6. *a*) Arrhenius plot (k_{kin} numbers in $\log_{10}$ scale) for reduction of N_2O by reaction with coal char [12] of various origin. The lowest reactivity corresponds to high-temperature bituminous coal coke, the highest reactivities correspond to lignite chars (——). *b*) N_2O reduction over (ash + sand) material from a circulating fluidized bed combustor at different CO volume fractions [35] at two different temperatures. Inlet N_2O volume fraction: 400 ppm.

Table 6. Comparison of Kinetic Constants, Pre-Exponential Factors, and Activation Energies for Reduction of N_2O by Chars and CO with Catalytic Decomposition of N_2O over Lime, Ash and with Homogeneous Reaction of N_2O Decomposition

Material	Pre-Exponential factor A	Activation energy E_a/(kJ mol^{-1})	Kinetic constant k_{kin} at 1123 K	Ref.
Cedar grove char	267 × T/K	115.5	1.3 m^3 kg^{-1} s^{-1}	[33]
Eschweiler char	41.6 × T/K	83	6.3 m^3 kg^{-1} s^{-1}	[33]
Reaction with CO (1 vol. %)	8.2 × 10^6 *	163 *	0.1 m^3 kg^{-1} s^{-1} *	[34]
CFBC ash material (with CaO, $CaSO_4$)	32	57	0.07 m^3 kg^{-1} s^{-1}	[36]
FBC ash	1.5 × 10^6	180	6.3 × 10^{-3} m^3 kg^{-1} s^{-1}	[31]
Peat ash	5.3 × 10^8	212.8	0.064 m^3 kg^{-1} s^{-1}	[33]
Calcined limestone	4.3 × 10^3	68.2	2.9 m^3 kg^{-1} s^{-1}	[31]
Calcined limestone (chalk)	1.3 × 10^6	110	9.94 m^3 kg^{-1} s^{-1}	[31]
Homogeneous thermal N_2O decomposition	4.2 × 10^9	224.5	0.15 s^{-1}	[33]

*In the case of N_2O-catalyzed reaction with CO the kinetic constant k_{kin} in Table 6 was calculated using "adsorption" kinetic expression [34]

$$k_{kin} = k_0 \cdot \exp(-E_a/RT) \cdot c_{CO}/(k_2 + c_{CO}) \qquad (13)$$

where the constant k_2 was considered [34] to be 0.3 mol m^{-3}.

the activity practically disappears. The reduction of catalytic activity of a calcined lime due to higher CO_2 partial pressure can be described by the equation

$$-r(N_2O) = k_1(T)c(N_2O)/(k_2(T) + c(CO_2)) \qquad (12)$$

where $k_1(T)$ and $k_2(T)$ are temperature-dependent constants specific for various limestones [31]. Some inorganic reducing compounds (*e.g.* CaS) react (as gas—solid noncatalyzed reaction) with N_2O.

Reduction of Nitrous Oxide

The main and the most important heterogeneous reduction reactions of N_2O in practical combustion system are reactions with char C, CO, H_2, C_xH_y, Fe_3O_4, and CaS. The reaction of N_2O with a char C in combustion systems, treated often as a pseudo-first-order reaction with respect to N_2O, with the reaction mechanism

$$N_2O + (—C) \rightarrow N_2 + (—CO) \qquad (P)$$

is always less or more accompanied by char C catalyzed reaction between N_2O and CO. The reaction rate of N_2O reduction is faster (approximately by an order of magnitude) than the reduction of NO with char C.

The Arrhenius plot for N_2O reduction over various chars is shown in Fig. 6*a*. The activities of high-temperature coke char on one hand and lignite char and active, wood-derived char on the other one differ by roughly an order of magnitude [12] in the temperature range 1000—1200 K. The variation in activation energies for the reaction (*10*) is [9, 12] 80—200 kJ mol^{-1} at lower temperatures and decreases to a range 66—130 kJ mol^{-1} with increasing temperature (influence of pore diffusion at $T > 1100$ K). The activation energies for reaction of NO with char C are 110—190 kJ mol^{-1}.

The pre-exponential factors, activation energies,

and computed values (for 1123 K) of kinetic constant for N_2O decomposition and reduction over char, calcined limestone, ash and homogeneous decomposition of N_2O are compared in Table 6.

Mechanism of char-C reaction with N_2O (Table 6) is changing in broader temperature range. This is the main reason for frequently used practical approximation of experimental kinetics data by frequency (pre-exponential) factor as a linear function of temperature in reaction rate equations for combustion and emission formation at high temperatures.

The experimentally measured values of the rate constant for N_2O reduction by char depend on char particle size ($\boldsymbol{k}_{\mathbf{kin}} \propto 1/(d_p)^{0.6-0.8}$) or more precisely on specific surface of particles. The reason is that the *in situ* measurement of surface of reacting particles at high temperature is difficult. Most such kinetic measurements are related to mass of char and not to surface of char. Generally, the larger char particles (*i.e.* lower specific surface of particles) the lower values of kinetic rate constant (related to mass of char) are observed [34].

Reaction of CO with N_2O is catalyzed by ash, calcined limestone, and by some other materials. The reaction mechanism involves fast reversible chemisorption of CO and irreversible reaction of N_2O with the sorbed CO

$$\mathrm{CO} + (\mathrm{—C}) \rightleftharpoons (\mathrm{—CO}) \qquad (Q)$$

$$\mathrm{N_2O} + (\mathrm{—CO}) \rightarrow \mathrm{N_2} + \mathrm{CO_2} + (\mathrm{—C}) \qquad (R)$$

From the above reaction scheme it is clear that reaction (P) may accompany even the "direct" reduction of N_2O by a char. Suitable kinetic expression for the catalyzed CO—N_2O reaction is of the Langmuir—Hinshelwood type, *e.g.*

$$-r(\mathrm{N_2O}) = k_1 \cdot c(\mathrm{N_2O}) \cdot c(\mathrm{CO}) /$$

$$(1 + K_1 \cdot c(\mathrm{N_2O}) + c(\mathrm{CO_2})/K_2 + K_3 \cdot c(\mathrm{CO})) \quad (14)$$

where k_1, K_1, K_2, and K_3 are kinetic constants and ratios of kinetic constants. If only sorption of CO is important, eqn (*14*) can be rewritten to a kinetic expression

$$-r(\mathrm{N_2O}) \approx k_2 \cdot c(\mathrm{N_2O}) \cdot c(\mathrm{CO})/(k_3 + c(\mathrm{CO})) =$$

$$= \boldsymbol{k}_{\mathbf{kin}} \cdot c(\mathrm{N_2O}) \qquad (15)$$

where the constant $\boldsymbol{k}_{\mathbf{kin}}$ is identical with $\boldsymbol{k}_{\mathbf{kin}}$ in eqn (*13*).

The measured kinetic data on reduction of N_2O by CO catalyzed *e.g.* by coal ash from FBC follow such trend (*i.e.* decreasing reaction order with respect to CO from 1 at low CO volume fractions (< 1 %) to practically zero at CO volume fractions ≧ 2.5 %) as illustrated in Fig. 6*b*. The computed values of kinetic constant $\boldsymbol{k}_{\mathbf{kin}}$, activation energy, and pre-exponential factor for the N_2O—CO ash-catalyzed reaction are compared with other N_2O decomposition reactions in Table 6.

N_2O reduction by H_2 (or by a mixture N_2O + CO + H_2O producing hydrogen) catalyzed by char or ash surfaces is a very fast reaction [36]. The reduction rate is substantially higher than in the case of the N_2O—CO reaction. In the presence of oxygen, CO and H_2 are oxidized primarily by oxygen and the reduction reaction rate decreases [36]. The heterogeneous reduction and decomposition reactions of N_2O are significant at higher char and CaO particle concentrations in systems with lower temperature of combustion (*e.g.* fluidized bed combustion) [33—35].

Fluidized Bed Combustion as Significant Source of N_2O Emissions

Coal combustion technologies produce N_2O emissions mainly as a consequence of lower combustion temperatures. Fluidized bed combustion (FBC) technologies due to necessity of the *in situ* desulfurization by limestone addition typically have operating temperatures between 800 °C and 900 °C. The combustion temperature in FBC is dictated by thermal output (load). At lower thermal output the combustion temperatures decrease and N_2O emissions increase. The situation is schematically shown in Fig. 7. It is clear that any circulating FBC unit should be operated in an "optimum" thermal load (at temperatures 850—900 °C) to avoid higher emissions of gaseous pollutants (N_2O, CO, NO or SO_2).

The N_2O emissions from FBC units depend on coal rank. Generally higher N_2O emissions were measured in combustion of bituminous, higher rank coals than in combustion of lignite and subbituminous coals.

Primary to secondary air ratio (air staging) in FBC is a very efficient tool for minimization of NO_x emissions. Influence of air splitting on N_2O emissions is, however, weaker [36, 37].

The heterogeneous (catalyzed) decomposition and reduction reaction of N_2O are very characteristic of fluidized bed combustion. Especially char and calcined limestone load in fluidized bed cause destruction of N_2O. Modelling of emissions from a fluidized bed combustor can distinguish [38] contributions of reactions in bubble (gas voids) and "emulsion" (particulate) phase for N_2O formation and destruction. As an example, effect of fluidized bed temperature and operating pressure on N_2O emission from FBC using detailed kinetic modelling [38] is given in Fig. 8.

In high-temperature pulverized combustion of coal the emissions of N_2O are negligible due to high temperature and in combustion of peat, wood, and biomass due to the high content of volatile matter and

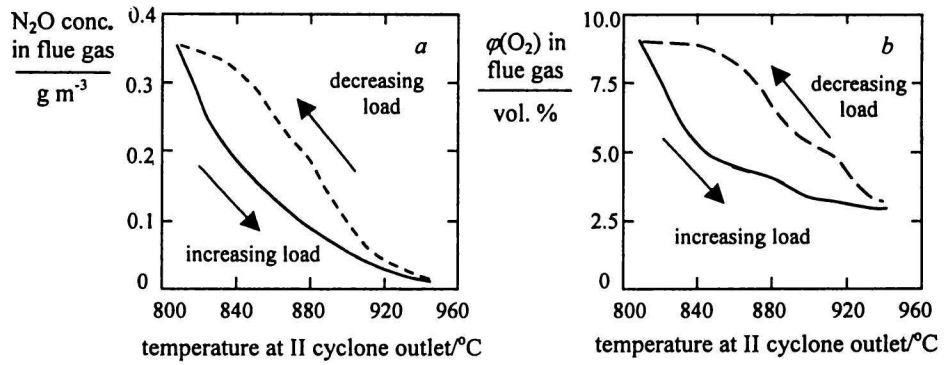

Fig. 7. N_2O emission behaviour of a 200 MW circulating fluidized bed combustion unit as a function of the flue gas temperature under decreasing and increasing thermal load [36]. *a*) Emissions of N_2O; *b*) flue gas oxygen concentrations.

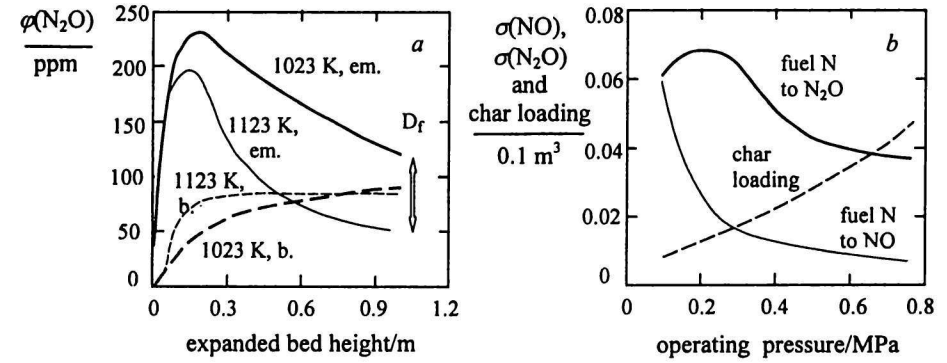

Fig. 8. Modelling of emissions from FBC of coal. Fluidized bed diameter 4 m, bed height at incipient fluidization 0.75 m, bed particle size range 0.2—5 mm, combustion of a bituminous coal with 1.2 mass % N and 67 mass % C [38]. *a*) Effect of fluidized bed temperature on N_2O emissions from bubbles (b.) and emulsion (em.) phase of the fluidized bed. D_f = destruction of N_2O due to the increased char—N_2O reaction rate. em. = "emulsion phase" of fluidized bed, b. = "bubble phase" of fluidized bed. *b*) Effect of operating pressure on fuel-N conversion to NO and N_2O inside the fluidized bed and dependence of fluidized bed char loading on the pressure.

water vapour leading to negligible formation of HCN in pyrolysis/gasification stage of devolatilization and combustion.

CONCLUSION

The heterogeneous reactions in combustion of solid fuels (devolatilization, formation of NO/N_2O emission precursors NH_3 + HCN, catalyzed oxidation of HCN to N_2O, catalyzed reactions of NO with reducing gases like HCN, CO, H_2, *etc.*, reduction of N_2O by CO and H_2, gas—solid reaction of N_2O with solid carbon and catalytic decomposition of N_2O) play a very important role in formation and destruction of N_2O emissions. The prevailing precursor of N_2O in combustion is HCN. At lower combustion temperatures, under higher H_2O vapour concentrations and in combustion of lignite coals and biomass, NH_3 is the main nitrogen oxide (NO + N_2O) precursor.

At temperatures 800—900 °C the catalyzed oxidation reaction of HCN is much faster than the homogeneous corresponding reaction. The selectivity for N_2O formation from volatile N (HCN) catalytic oxidation is 2—10 % for lignite coals and 10—30 % for anthracitic, high-rank coals. The conversions decrease with increasing combustion temperature. Efficient catalysts for the oxidation reactions are char, calcined limestone, and coal ash.

Oxidation of coal-char nitrogen to N_2O generally increases with increasing carbon conversion (burnout). The destruction (reduction) reactions of N_2O are coupled mainly with the presence of char carbon, CO, and H_2 (H_2O). N_2O formation in char combustion may follow various mechanisms (direct oxidation of char N, reaction of char N with NO, and homogeneous oxidation of HCN released from a char).

Reactive chars with developed rich porous structure and high specific pore surface area (*e.g.* from lignite and subbituminous coals) are very efficient in NO and N_2O *in situ* reduction. CaO, metallic oxides, zeolites, and petrovskite oxide mixtures were recognized and proved [4, 5] to be the most common catalysts for decomposition of N_2O under medium and higher temperatures (400—800 °C).

Increasing operating temperature, increasing pressure, higher CO concentrations, and higher char load lead in combustion systems (*e.g.* in FBC) to lower emissions of N_2O. The emissions of N_2O in staged FBC do not exceed (at temperatures over 850 °C) 200 mg m^{-3} for bituminous and anthracitic coals and 100 mg m^{-3} for lignite coals. Very efficient method for reduction of N_2O emission is reburning (additional combustion) of natural gas or of a solid, high volatile content fuel (like sawdust) in or after the cyclone separator [35, 39].

Combustion processes with temperatures over 1000 °C (*e.g.* pulverized coal combustion) are only insignificant source of N_2O emissions due to the thermal destruction of N_2O.

Acknowledgements. The authors appreciate financial support from the Grant Agency of the Academy of Sciences of the Czech Republic (Project No. A 407 2801).

SYMBOLS

A	frequency factor	s^{-1}
c	concentration	mol m^{-3}
$c(N_T)$	total active site concentration of nitrogen per volume unit of catalyst in eqn (*10*)	mol m^{-3}
(—C)	active site on carbon (char) surface	
(—CO)	active site-surface complex containing oxygen	
(—CN), (—CNO)	active site-surface complexes containing nitrogen and (oxygen + nitrogen)	
conv.	conversion of a species (*e.g.* HCN) to products (N_2 + NO + N_2O)	
d_p	diameter of solid particles	m
daf	dry, ash-free conditions for coals	
E_a	activation energy of reaction	kJ mol^{-1}
k, k_{kin}	kinetic rate constant [s^{-1} for the 1st-order reactions; mol m^{-3} s^{-1} for the 2nd-order reactions; m^3 kg^{-1} s^{-1} for catalytic reactions, or as given in the text of the paper]	
$\boldsymbol{k_i}$	rate constant for pyrolysis and decompositions according to eqn (*1*), *i.e.* pseudo-Arrhenius rate constant	s^{-1}
$\boldsymbol{k_{kin}}$	"complex" kinetic rate constant in eqns (*13*) and (*15*)	s^{-1}
m	mass	kg
$n(Y)$	amount of substance of species Y	mol
p_i, $p(i)$	partial pressure of species i	Pa
P	total pressure	Pa
$r(Y)$	net rate of formation for species Y	mol m^{-3} s^{-1}
$r_v(Y)$	net rate of formation of a product in Table 3 (units given in Table 3)	
$\boldsymbol{R}$	gas constant = 8.31433 J mol^{-1} K^{-1}	
S	sum of all active sites in a char, defined by eqn (*5*)	mol
T	absolute temperature	K
t	time	s
V	volume	m^3
W_{0i}	ultimate (total) mass yield of product (or gas) "i" from mass unit of coal or char i	
W_i	the mass of "i" already evolved from mass unit of coal or gas (eqn (*1*))	
$w(V^{daf})$	mass fraction of volatiles in coal for daf conditions	
$w(C^{daf})$	mass fraction of carbon in coal for daf conditions	
$w(H^{daf})$	mass fraction of hydrogen in coal for daf conditions	
$w(O^{daf})$	mass fraction of oxygen in coal for daf conditions	
$w(N^{daf})$	mass fraction of nitrogen in coal for daf conditions	
$x_r(Y)$	relative mole fraction of solid species Y ("surface concentration") n/n(solid)	
x_S	mole fraction of individual active sites defined in eqn (*4*)	
x_A, x_O, x_{N_2O}	mole fraction of A*, O*, and N_2O* in eqn (*10*)	
φ	volume fraction	
ψ	mole ratio [n(N)/n(C)]	
σ(NO)	selectivity for NO formation by oxidation of HCN or NH_3 (moles of NO formed by HCN or NH_3 oxidation/moles of HCN or NH_3 oxidized)	
$\sigma(N_2O)$	selectivity of N_2O formation by oxidation of HCN or NH_3	
θ	temperature	°C

REFERENCES

1. Kramlich, J. C. and Linek, W. P., *Prog. Energy Combust. Sci. 20*, 149 (1994).
2. Mann, M. D., Collings, M. E., and Botros, P., *Prog. Energy Combust. Sci. 18*, 447 (1992).
3. Arai, N., *J. Inst. Energy 67*, 61 (1994).
4. Svoboda, K., Hartman, M., and Veselý, V., *Chem. Listy 88*, 13 (1994).
5. Kaptein, F., Rodriguez-Mirasol, J., and Moulijn, J. A., *Appl. Catal., B 9*, 25 (1996).
6. Pires, M., van den Bergh, H., and Rossi, M. J., *J. Atmos. Chem. 25*, 229 (1996).
7. Hämäläinen, J. P., Aho, M. J., and Tummavuori, J. L., *Fuel 73*, 1895 (1994).
8. Saastomoinen, J. K., Aho, M. J., and Linna, V. L., *Fuel 72*, 599 (1993).
9. Thomas, K. M., *Fuel 76*, 457 (1997).
10. Middleton, S. P., Patrick, J. W., and Walker, A., *Fuel 76*, 1195 (1997).
11. Johnsson, J. E., *Formation of Volatile Nitrogen Compounds during Coal Pyrolysis and Devolatilization.* 26th IEA-AFB Meeting, San Diego, California, May 6, 1993.
12. Johnsson, J. E., *Fuel 73*, 1398 (1994).
13. Jensen, A., Johnsson, J. E., and Dam-Johansen, K., *AIChE J. 43*, 3070 (1997).
14. Leppälahti, J., *Fuel 74*, 1363 (1995).

15. Hämäläinen, J. P. and Aho, M. J., *Fuel 75*, 1377 (1996).
16. Kurkela, E. and Stählberg, P., *Fuel Process. Technol. 31*, 23 (1992).
17. Solomon, P. R., Serio, M. A., and Suuberg, E. M., *Prog. Energy Combust. Sci. 18*, 133 (1992).
18. Hulgaard, T., *Ph.D. Thesis.* Technical University of Denmark, Lyngby, 1991.
19. Schäfer, S., Bonn, B., and Baiman, H., *Proc. of the Int. Conf. on Coal Sci.* (Edited by Ziegler, A. *et al.*) Essen, Germany, Sept. 1997. DGMK Tagungsberichte 9703, pp. 1091—1094.
20. Jensen, A., *Ph.D. Thesis.* Technical University of Denmark, Lyngby, 1996.
21. Shimizu, T., Ishizu, K., Kobayashi, S., Kimura, S., Shimizu, T., and Inagaki, M., *Energy Fuels 7*, 645 (1993).
22. Hayhurst, A. N. and Lawrence, A. D., *Combust. Flame 105*, 511 (1996).
23. Hayhurst, A. N. and Lawrence, A. D., *Combust. Flame 105*, 341 (1996).
24. Hulgaard, T. and Dam-Johansen, K., *AIChE J. 39*, 1342 (1993).
25. Feng, B., Liu, H., Yuan, J., Lin, Z., Liu, D., and Leckner, B., *Energy Fuels 10*, 203 (1996).
26. Miettinen, H., Paulsson, M., and Strömberg, D., *Energy Fuels 9*, 10 (1995).
27. Miettinen, H., *Energy Fuels 10*, 197 (1996).
28. Tullin, C. J., Sarofim, A. F., and Beer, J. M., *Proc. of the 12th Int. Conf. on Fluidized Bed Combustion*, pp. 599—609, San Diego, USA, 1993.
29. Mallet, C., Aho, M., Hämäläinen, J., Rouan, J. P., and Richard, J. R., *Energy Fuels 11*, 792 (1997).
30. Croiset, E., Heurtenbise, C., Rouan, J. P., and Richard, J. R., *Combust. Flame 112*, 33 (1998).
31. Johnsson, J. E., Jensen, A., Vaaben, R., and Dam-Johansen, K., *Proc. of the 14th Int. Conf. on Fluidized Bed Combustion*, Vol. *II*, pp. 953—966. Vancouver, Canada, May 11—14, 1997.
32. Li, Y. and Armor, J., *Appl. Catal., B 1*, L 21 (1992).
33. Amand, L. E. and Leckner, B., *Fuel 73*, 1389 (1994).
34. Johnsson, J. E., Amand, L. E., Dam-Johansen, K., and Leckner, B., *Energy Fuels 10*, 970 (1996).
35. Gustavsson, L., Glarborg, P., and Leckner, B., *Combust. Flame 106*, 345 (1996).
36. Bonn, B., Pelz, G., and Bauman, H., *Fuel 74*, 165 (1995).
37. Diego, L. F., London, C. A., Wang, X. S., and Gibbs, B. M., *Fuel 75*, 971 (1996).
38. Goel, S. K., Beer, J. M., and Sarofim, A. F., *J. Inst. Energy 69*, 201 (1996).
39. Rutar, T., Kramlich, J. C., and Malte, P. C., *Combust. Flame 107*, 453 (1996).